



# TEMPO-mediated oxidation of $\beta$ -chitin to prepare individual nanofibrils

Yimin Fan, Tsuguyuki Saito, Akira Isogai \*

Graduate School of Agricultural and Life Sciences, The University of Tokyo, Tokyo 113-8657, Japan

## ARTICLE INFO

### Article history:

Received 26 November 2008

Received in revised form 13 February 2009

Accepted 2 March 2009

Available online 11 March 2009

### Keywords:

$\beta$ -Chitin  
TEMPO  
Crystallinity  
Nanofibril  
Tubeworm

## ABSTRACT

TEMPO (2,2,6,6-tetramethylpiperidine-1-oxyl radical)-mediated oxidation was applied to  $\beta$ -chitins, originating from tubeworm and squid pen, to prepare chitin nanofibrils. Water-insoluble fractions of the TEMPO-oxidized  $\beta$ -chitins were obtained in various ratios by controlling the addition level of NaClO used as the primary oxidant in the oxidation. The water-insoluble fractions of the TEMPO-oxidized tubeworm  $\beta$ -chitins, when they had carboxylate groups of 0.18–0.25 mmol/g, were successfully converted to highly viscous and translucent gels by disintegration in water. The gels consisted of mostly individual nanofibrils 20–50 nm in width and at least several microns in length. On the other hand, the water-insoluble fractions of the TEMPO-oxidized squid pen  $\beta$ -chitins could be transformed to neither transparent nor translucent dispersions under any oxidation or disintegration conditions used. When sufficient amounts of NaClO were used, both  $\beta$ -chitins were completely oxidized to the corresponding water-soluble polyuronic acids by oxidation of all C6 primary hydroxyls to carboxylate groups.

© 2009 Elsevier Ltd. All rights reserved.

## 1. Introduction

Chitins are present in the outer shells of crustaceans such as crab and shrimp, the cuticles of insects and the cell walls of some fungi. Isolated chitins are linear and crystalline hetero-polysaccharides consisting of *N*-acetylanhydroglucosamine and anhydroglucosamine units with various ratios linked by  $\beta$ -(1  $\rightarrow$  4)-glycoside bonds. Native chitins consist of crystalline fibrils, whose lateral dimensions range from 2.5 to 50 nm, depending on their biological origins (Revol & Marchessault, 1993). Thus, chitins have potential to be converted to nanofibrils to be used as highly functional materials by so-called downsizing processes (Goodrich & Winter, 2007; Lu, Weng, & Zhang, 2004; Muzzarelli et al., 2007; Paillet & Dufresne, 2001; Revol & Marchessault, 1993).

We have developed new methods to prepare individual and highly crystalline cellulose nanofibrils dispersed in water from native celluloses by 2,2,6,6-tetramethylpiperidine-1-oxyl radical (TEMPO)-mediated oxidation and the following mild mechanical treatment (Saito et al. 2006, 2007). The formation of C6 carboxylate groups on the cellulose microfibril surfaces by the TEMPO-oxidation is the key factor for preparation of the cellulose nanofibrils. Electrostatic repulsion and/or osmotic effect due to anionically charged carboxylate groups formed on the cellulose microfibril surfaces in the inter-fibrillar layers can overcome numerous hydrogen bonds originally present between microfibrils in native cellulose fibers (Saito et al., 2007).

When the TEMPO-mediated oxidation with sufficient amounts of NaClO used as the primary oxidant is applied to crab shell  $\alpha$ -chitins, the corresponding water-soluble polyuronic acid Na salts can be obtained by the regioselective oxidation of the C6 primary hydroxyl groups to carboxylate groups (Kato, Kaminaga, Matsuo, & Isogai, 2004; Muzzarelli, Muzzarelli, Cosani, & Terbojevich, 1999). On the other hand, when the amount of NaClO added was controlled or reduced, water-insoluble fractions of the TEMPO-oxidized  $\alpha$ -chitins are obtained in various yields, depending on the oxidation conditions. Transparent and homogeneous dispersions can be obtained by mild disintegration of the water-insoluble TEMPO-oxidized  $\alpha$ -chitins in water, when they are prepared under specifically designed conditions. The dispersions consist of nano-whiskers with average width and length of 8 nm and 340 nm, respectively (Fan, Saito, & Isogai, 2008a). The driving force to prepare TEMPO-oxidized  $\alpha$ -chitin nano-whiskers is electrostatic repulsion and/or osmotic effect between anionically charged chitin fibrils of TEMPO-oxidized  $\alpha$ -chitins in a similar manner to those for TEMPO-oxidized cellulose nanofibrils.

Based on the above principle to prepare cellulose nanofibrils, individual chitin nanofibrils 3–4 nm in cross-sectional width and at least a few microns in length were successfully prepared from squid pen  $\beta$ -chitin by simple mechanical disintegration in acidic water at pH 3–5 (Fan, Saito, & Isogai, 2008b). In this case, surface cationic charges are formed at the glucosamine units on the fibril surfaces, which then bring about the inter-fibrillar electrostatic repulsion in water. Thus, the opposite charges to TEMPO-oxidized cellulose nanofibrils are formed on the surfaces of squid pen  $\beta$ -chitin fibrils in this case. The relatively low crystallinity and hydrated crystal form of squid pen  $\beta$ -chitin (Mazeau, Winter, & Chanzy,

\* Corresponding author. Tel.: +81 3 5841 5538; fax: +81 3 5841 5269.  
E-mail address: [aisogai@mail.ecc.u-tokyo.ac.jp](mailto:aisogai@mail.ecc.u-tokyo.ac.jp) (A. Isogai).

1994) might be necessary factors to prepare the nanofibrils by the above simple method.

Other than squid pen, tubeworms and diatoms have  $\beta$ -chitins, whose crystallinity indices and degrees of N-acetylation are much higher than those of squid pen  $\beta$ -chitin (Kurita, 2001; Muzzarelli, 1977). Despite squid pen  $\beta$ -chitin, the tubeworm  $\beta$ -chitin could not be converted to individual nanofibrils by the mechanical disintegration in acidic water under any conditions, probably because of the quite small amount of C2 amino groups as well as the high crystallinity (Fan et al., 2008b). Thus, TEMPO-mediated oxidation is rather better process for tubeworm  $\beta$ -chitin to be converted to individual and highly crystalline nanofibrils dispersed in water, just like the case of native celluloses.

In this study, therefore, TEMPO-mediated oxidation was applied to tubeworm and squid pen  $\beta$ -chitins to form C6 carboxylate groups just on the fibril surfaces and to obtain water-insoluble oxidized products in high yields by controlling the oxidation conditions. The water-insoluble fractions, when obtained, may have potential to be converted to individual and highly crystalline nanofibrils by mild disintegration in water.

## 2. Materials and methods

### 2.1. Materials

Tubeworm (*Lamellibrachia satsuma*) and pens of squid (*Todarodes pacificus*) were used as resources of highly and low crystalline  $\beta$ -chitins, respectively. The  $\beta$ -chitins were purified, according to the conventional procedure (Li, Revol, & Marchessault, 1997), and stored as never-dried samples at 4 °C before use. The crystallinity indices of the tubeworm and squid pen  $\beta$ -chitins, calculated from X-ray diffraction patterns (see the following analysis section), were 0.74 and 0.51, respectively (Fan et al., 2008b). The degrees of N-acetylation of tubeworm and squid pen  $\beta$ -chitins, which were calculated from their carbon and nitrogen contents were 0.99 and 0.90, respectively. TEMPO, sodium bromide, 2 M sodium hypochlorite solution, and other chemicals and solvents were of laboratory grade (Wako Pure Chemicals, Co., Japan), and used without further purification.

### 2.2. TEMPO-mediated oxidation

TEMPO-mediated oxidation was carried out to the  $\beta$ -chitins, basically according to the same procedure as for crab shell  $\alpha$ -chitin (Fan et al., 2008a). The purified and never-dried  $\beta$ -chitin (1 g, dry weight) was suspended in water (100 ml) containing TEMPO (0.016 g, 0.1 mmol) and sodium bromide (0.1 g, 1 mmol). The oxidation of chitin was started by adding a designed amount of the NaClO solution (0–20 mmol NaClO per gram of chitin). The pH of the slurry was maintained to be 10 at room temperature by continuous addition of 0.5 M NaOH using a pH stat. When no consumption of the alkali was observed, the oxidation was quenched by adding a small amount of ethanol to the mixture. After the pH was adjusted to 7 with 0.5 M HCl, the mixture was centrifuged at 12,000 gravity for 5 min, and the supernatant was removed by decantation. The water-insoluble fraction thus obtained was washed thoroughly with water by repeated centrifugation and the successive decantation of the supernatant. A part of the water-insoluble fraction was freeze-dried for analyses, and the rest was stored at 4 °C as a never-dried TEMPO-oxidized chitin sample before use.

### 2.3. Analyses of the water-insoluble fractions of TEMPO-oxidized $\beta$ -chitins

The C6 carboxylate contents of the TEMPO-oxidized chitins were determined from conductivity titration curves and contents

of the C2 amino groups determined beforehand by FT-IR method (Fan et al., 2008a). To a dried sample (0.2 g) were added water (60 mL) and a small amount of 0.5 M NaOH to adjust the suspension pH to 9. The suspension was stirred for 30 min to prepare sufficiently dispersed slurry. Then, 0.1 M HCl was added to the slurry to set the pH 2.5–3.0. A 0.05 M NaOH solution was added at a rate of 0.1 mL/min up to pH 11 using a pH-stat titration system. The conductivity and pH curves thus obtained contribute to the contents of both carboxylate and C2 amino groups in the TEMPO-oxidized chitins. Hence, the carboxylate content was obtained by subtracting the content of amino groups determined beforehand from the titration value. To a freeze-dried TEMPO-oxidized chitin (0.5 g), were added water (40 mL), NaClO<sub>2</sub> (0.9 g) and 5 M acetic acid (5 mL), and the mixture was stirred at room temperature for 48 h to selectively oxidize aldehyde groups in the samples to carboxylate groups at pH 4–5. The NaClO<sub>2</sub>-oxidized samples were washed thoroughly with water by filtration or centrifugation, and carboxylate contents were determined by the aforementioned method. The carboxylate groups formed by the NaClO<sub>2</sub> oxidation were regarded as aldehyde groups in the original TEMPO-oxidized chitins.

The freeze-dried chitin samples were converted to pellets using a disk apparatus for IR measurement, and subjected to X-ray diffraction analysis from 5° to 35° of diffraction angle  $2\theta$  using the reflection method by means of a Rigaku RINT 2000 with a Ni-filtered CuK $\alpha$  radiation ( $\lambda = 0.1548$  nm) at 40 kV and 40 mA. The crystallinity indices of  $\beta$ -chitins based on the  $2\theta$  scan from 5° to 35° were calculated accorded to the method reported by Li et al. (1997), which requires separation of the crystalline peaks from the diffuse background. The crystal size to the (100) direction was measured from the full width at half-height of the diffraction peak (010) using Scherrer's equation (Alexander, 1979).

Solid-state <sup>13</sup>C-NMR spectra of samples were recorded with a Bruker Avance spectrometer operated at 100 MHz for the <sup>13</sup>C nucleus. The spectra were acquired at room temperature with a 80 kHz proton dipolar decoupling field, matched cross-polarization (CP) fields of 80 kHz, a proton 90° pulse of 2.5  $\mu$ s and magic angle spinning (MAS) at a spinning rate of 12 kHz (Peersen, Wu, Kustanovich, & Smith, 1993). The repetition time was 4 s, and the average number of 20,000 scans was acquired for each spectrum.

FT-IR spectra of the original and TEMPO-oxidized chitins were recorded with 4 cm<sup>-1</sup> resolution and 64 scans on a Nicolet Magna 860 (Madison, WI, USA) in the transmission mode. Here, the original  $\beta$ -chitins were converted to KBr disks for FT-IR analysis. The TEMPO-oxidized chitin/water dispersions were cast on a Teflon plate followed by drying overnight at 50 °C. The dried films were then treated with 0.1 M HCl to convert the sodium carboxylate groups to free carboxyls followed by vacuum-drying at 60 °C for 24 h. The dried thin films were subjected to FT-IR analysis.

### 2.4. Disintegration of the water-insoluble TEMPO-oxidized $\beta$ -chitins in water

The water-insoluble fraction of the TEMPO-oxidized  $\beta$ -chitin (never-dried form) was suspended in water at 0.2% consistency. The slurry (10 ml) was first disintegrated by a blender-type homogenizer at 15,000 rpm for 2 min (Excel Auto EO-4, Nihonseiki, Japan), and then treated by an ultrasonic homogenizer at 19.5 kHz and the 300 W output power (7 mm in the probe tip diameter, US-300T, Nihonseiki, Japan) for 1 min at room temperature.

### 2.5. Analyses of the TEMPO-oxidized $\beta$ -chitin dispersions

$\zeta$ -Potentials of  $\beta$ -chitin components dispersed in water at 0.01% (w/v) consistency were measured at 20 °C using a laser-Doppler-electrophoresis-type apparatus (DTS5300 Zetasizer 3000, Malvern Instruments, UK). The transmittances of the 0.1% TEMPO-oxidized

chitin dispersions were measured from 300 to 700 nm using a Shimadzu UV–vis spectrophotometer (UV-1700). A 10  $\mu$ l aliquot of the 0.02% (w/v) TEMPO-oxidized chitin/water dispersion was mounted on a glow-discharged carbon-coated electron microscopy grid. After drying, the sample grid was observed at 100 kV using a JEOL transmission electron microscope (JEM 2000-EXII) (Fan, Saito, & Isogai, 2008a, 2008b). The fibril images were taken at diffraction contrasts in the bright-field mode using a low-dose exposure, and the micro-diffraction technique was used in some cases (Imai, Watanabe, Yui, & Sugiyama, 2003). All micrographs were collected with a CCD camera (Keen View, Olympus Soft Imaging Solutions, Germany) and recorded using iTEM<sup>®</sup> software provided by the CCD camera company.

### 3. Results and discussion

#### 3.1. Carboxylate and aldehyde groups in the TEMPO-oxidized $\beta$ -chitins

Fig. 1 shows the relationships between the amount of NaClO added as the primary oxidant in the TEMPO-mediated oxidation and either weight ratio of the water-insoluble fraction or its carboxylate and aldehyde contents for tubeworm and squid pen  $\beta$ -chitins. The weight ratios of the water-insoluble fractions were decreased with increasing the amount of NaClO added. All water-soluble fractions consisted of chitouronic acids, whose C6 positions were completely oxidized to carboxylate groups, which were confirmed by their solution-state <sup>13</sup>C-NMR spectra (Fan et al., 2008a; Kato et al., 2004). Carboxylate contents in the water-insoluble fractions were increased with increasing the NaClO addition level up to about 5 mmol NaClO per gram of chitin, and then roughly reached plateau levels for both tubeworm and squid pen  $\beta$ -chitins. Thus, the weight ratios of the water-insoluble fractions and their carboxylate

contents can be controlled to some extent by controlling the amount of NaClO added in the TEMPO-mediated oxidation.

For example, when the NaClO addition level was 10.0 mmol/g, the weight ratios of the water-insoluble TEMPO-oxidized tubeworm and squid pen  $\beta$ -chitins were 71% and 49%, respectively. The contents of total oxidized groups (carboxylate + aldehyde groups) were 0.25 and 0.36 mmol/g, respectively. The higher crystallinity and larger crystal size (or smaller surface area) of tubeworm  $\beta$ -chitin might have resulted in such higher weight ratio of the water-insoluble fraction and smaller amounts of oxidized groups than for the squid pen  $\beta$ -chitin.

It is noteworthy that nearly no aldehyde groups were present in the TEMPO-oxidized tubeworm  $\beta$ -chitins, whereas both carboxylate and aldehyde groups were formed in similar ratios in the TEMPO-oxidized squid pen  $\beta$ -chitins. Thus, the aldehyde groups are likely to be formed in relatively disordered regions of squid pen  $\beta$ -chitins, and to present in the TEMPO-oxidized products forming hydrate or hemiacetal structures, which are highly resistant to further oxidation to carboxylate groups during the TEMPO-oxidation. On the other hand, no such aldehyde groups remain in the highly crystalline tubeworm  $\beta$ -chitin. This hypothesis may be applicable also to TEMPO-oxidized native celluloses, which have various aldehyde contents, depending on the cellulose origins (Saito & Isogai, 2004).

#### 3.2. Changes in crystallinity and crystal size of $\beta$ -chitins by TEMPO-mediated oxidation

X-ray diffraction patterns of the original and TEMPO-oxidized  $\beta$ -chitins are depicted in Fig. 2, and the relationships between the NaClO addition level and either crystallinity index or crystal size to the (100) direction of  $\beta$ -chitins are plotted in Fig. 3. The original crystal structures of  $\beta$ -chitins were intrinsically maintained in the water-insoluble fractions during the TEMPO-mediated oxidation. The diffraction peak due to the hydrate (010) space, which was originally present in the squid pen  $\beta$ -chitin around  $2\theta$  9° but not in the original tubeworm  $\beta$ -chitin (Blackwell, 1988; Saito, Kumagai, Wada, & Kuga, 2002), appeared in the TEMPO-oxidized tubeworm  $\beta$ -chitins.

Crystallinity indices were decreased for both  $\beta$ -chitins with increasing the NaClO addition level; disordered regions are formed

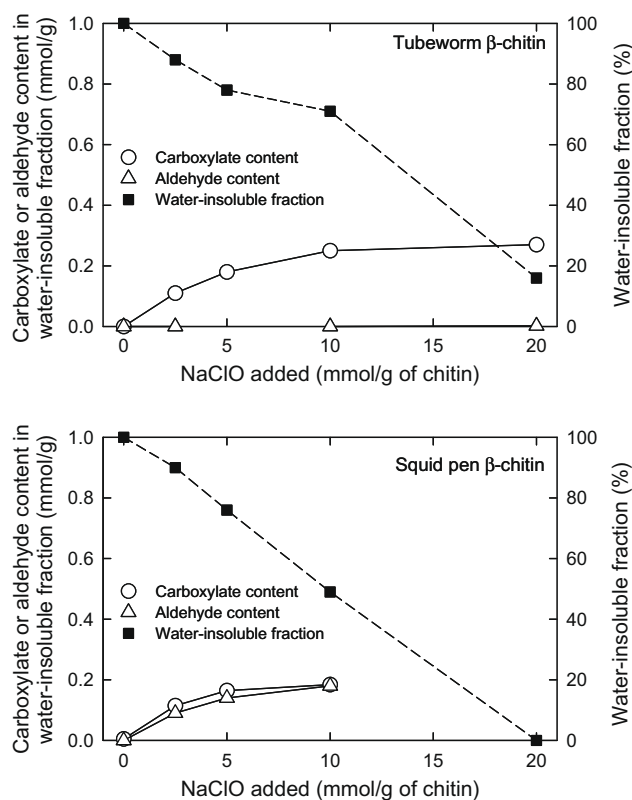


Fig. 1. Relationship between the NaClO addition level in the TEMPO-mediated oxidation of tubeworm and squid pen  $\beta$ -chitins and either weight ratio of water-insoluble fraction or its carboxylate and aldehyde contents.

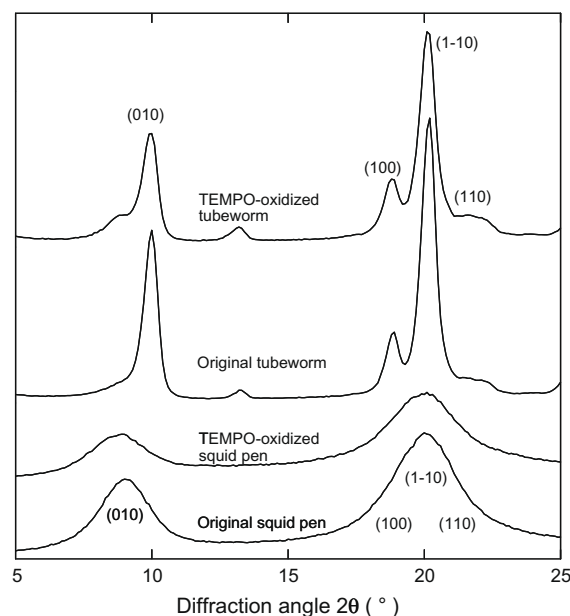
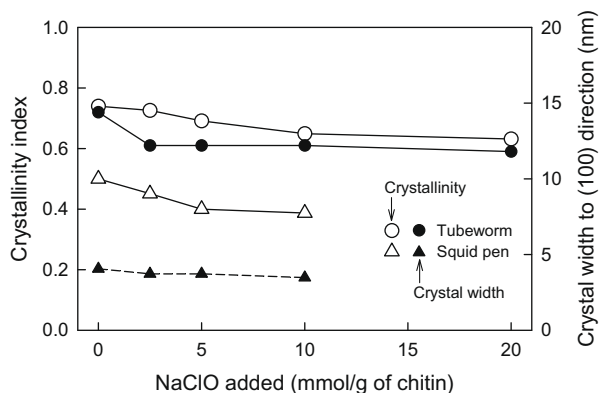


Fig. 2. X-ray diffraction patterns of the original  $\beta$ -chitins and their water-insoluble fractions of TEMPO-oxidized products prepared with 10 and 5 mmol NaClO per gram of tubeworm and squid pen  $\beta$ -chitins, respectively.



**Fig. 3.** Changes in crystallinity and the (100) crystal size of water-insoluble fractions of TEMPO-oxidized tubeworm and squid pen  $\beta$ -chitins prepared with various NaClO addition levels.

in the  $\beta$ -chitins to some extent by the oxidation. On the other hand, the crystal sizes to the (100) direction determined from the peak widths of (010) were mostly maintained by the oxidation. These results indicate that almost all carboxylate and aldehyde groups formed in the water-insoluble TEMPO-oxidized  $\beta$ -chitins are selectively present on the crystallite surfaces of  $\beta$ -chitins. Based on the results in Figs. 1 and 3, therefore, the remarkable decrease in the weight ratio of the water-insoluble fraction prepared with 20 mmol NaClO per gram of tubeworm  $\beta$ -chitin or with 10 mmol NaClO per gram of squid pen  $\beta$ -chitin in the oxidation might have been caused by significant decreases in the fibril lengths, not widths, of the original  $\beta$ -chitins during the TEMPO-mediated oxidation at these high NaClO addition levels. This subject will be further discussed in later.

### 3.3. Chemical structures of $\beta$ -chitins by TEMPO-mediated oxidation

Figs. 4 and 5 show solid-state  $^{13}\text{C}$ -NMR and FT-IR spectra, respectively, of the original  $\beta$ -chitins and the water-insoluble fractions of the TEMPO-oxidized  $\beta$ -chitins prepared with NaClO of 5 or 10 mmol/g. The patterns of the original solid-state  $^{13}\text{C}$ -NMR spectra were essentially unchanged even after the TEMPO-mediated oxidation. When the relative signal areas of C6 primary hydroxyls around 60 ppm to those of C1 around 103 ppm are compared before and after the oxidation, about 10–14% of the original signal areas due to the C6 primary hydroxyls decreased by the oxidation for both tubeworm and squid pen  $\beta$ -chitins. Inversely, the relative signal areas due to C=O signals around 176 ppm increased in both cases. Hence, the  $^{13}\text{C}$ -NMR results support that the carboxylate groups formed by the TEMPO-mediated oxidation originate from the C6 primary hydroxyls in the  $\beta$ -chitins. Moreover, the relative signal areas around 23 ppm due to acetyl amide carbons to those due to C1 carbons were nearly unchanged after the TEMPO-oxidation for both tubeworm and squid pen  $\beta$ -chitins, showing that no N-deacetylation occurred at the C2 positions of  $\beta$ -chitins during the oxidation.

FT-IR spectra also support the above conclusions. Carboxyl groups are formed in the  $\beta$ -chitins by the TEMPO-mediated oxidation, although the original crystal structures and degrees of N-acetylation are maintained (Morin & Dufresne, 2002; Shigemasa, Matsuura, Sashiwa, & Saimoto, 1996).

### 3.4. Disintegration of the water-insoluble TEMPO-oxidized $\beta$ -chitins in water

The water-insoluble TEMPO-oxidized tubeworm and squid pen  $\beta$ -chitins as well as the corresponding original  $\beta$ -chitins were

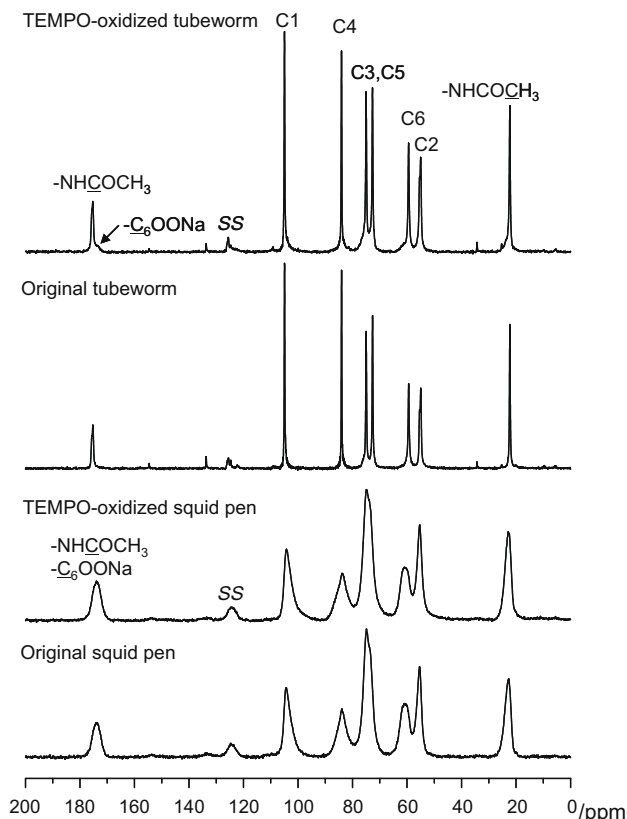


**Fig. 4.** Solid-state  $^{13}\text{C}$ -NMR spectra of the original  $\beta$ -chitins and their water-insoluble fractions of the TEMPO-oxidized products prepared with 10 and 5 mmol NaClO per gram of tubeworm and squid pen  $\beta$ -chitins, respectively. SS: spinning side band.

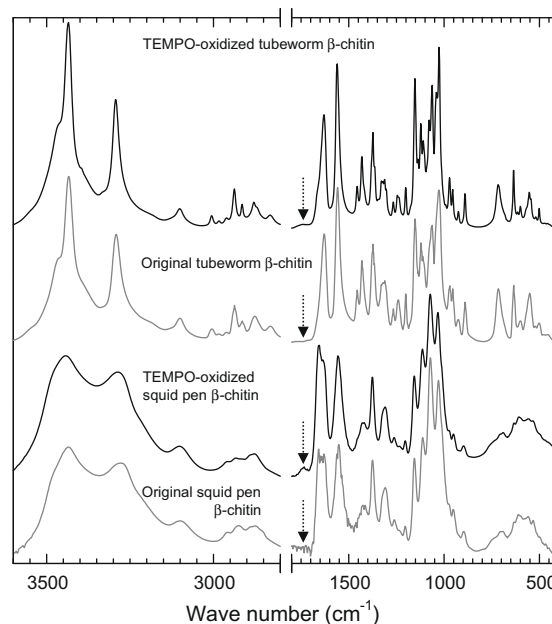


**Fig. 5.** FT-IR spectra of the original  $\beta$ -chitins and their water-insoluble fractions of TEMPO-oxidized products prepared with 10 and 5 mmol NaClO per gram of tubeworm and squid pen  $\beta$ -chitins, respectively. Arrows show the C=O band position due to carboxyl groups.

disintegrated in water. As shown in Fig. 6, the original squid pen  $\beta$ -chitin and its TEMPO-oxidized products prepared under any

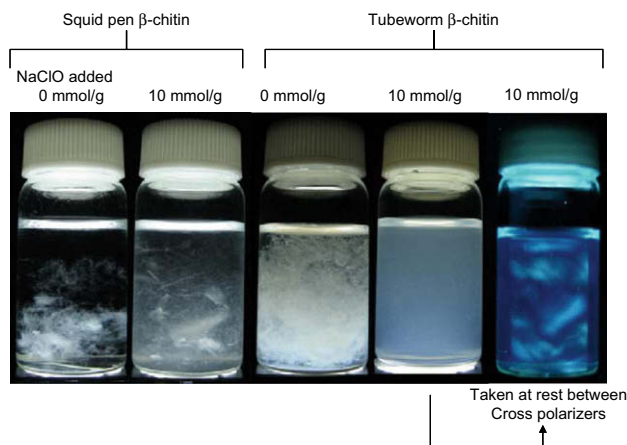


**Fig. 6.** Photographs of suspensions or dispersions of the original and TEMPO-oxidized  $\beta$ -chitins in water at 0.2% consistency.

conditions could not be converted to homogeneous dispersions even after extended disintegration time. Probably because numerous polyion complexes are formed between the amino groups present in the original squid pen  $\beta$ -chitin and the C6 carboxylate groups formed by the oxidation, individualization of fibrils could not be achieved in this case. The significant amounts of aldehyde groups formed by the oxidation and present in the water-insoluble TEMPO-oxidized squid pen  $\beta$ -chitins (Fig. 1) might also have caused such resistance to the conversion to individual fibrils, forming inter-fibrillar hemiacetal linkages between aldehyde groups formed and hydroxyls originally present in the  $\beta$ -chitin.

On the other hand, the water-insoluble fraction of the TEMPO-oxidized tubeworm  $\beta$ -chitin prepared with 10 mmol NaClO per gram of chitin homogeneously dispersed in water, providing a highly viscous and translucent gel (Fig. 6). The dispersion showed birefringence between cross polarizers, indicating that dispersed fibrils having optical anisotropy were stably present in the bottle.  $\zeta$ -Potentials of the TEMPO-oxidized tubeworm  $\beta$ -chitin components dispersed in water were around  $-60$  mV. Thus, the TEMPO-oxidized tubeworm  $\beta$ -chitin components had highly anionic charges due to carboxylate groups formed by the oxidation, and caused such stably dispersed state in water by electrostatic repulsion between the components. Because the original tubeworm  $\beta$ -chitin has a quite high degree of N-acetylation (0.99) or a quite low amount of C2 primary amino groups, the surface charges of the tubeworm  $\beta$ -chitin fibrils are governed by anionic charges due to the C6 carboxylate groups formed by the TEMPO-mediated oxidation rather than the amino groups slightly and originally present in the tubeworm  $\beta$ -chitin. Hence, the homogeneously dispersed state was obtained by disintegration of the water-insoluble TEMPO-oxidized tubeworm  $\beta$ -chitin in water, which was different from the results of the TEMPO-oxidized squid pen  $\beta$ -chitins.

Light transmittances of the 0.1% dispersions for the water-insoluble fractions of the TEMPO-oxidized tubeworm  $\beta$ -chitins prepared with different amounts of NaClO are shown in Fig. 7 together with their photographs. The light transmittance was increased as the NaClO addition level increased, showing that individualization of the tubeworm  $\beta$ -chitin fibrils was enhanced by the increased amounts of carboxylate groups formed in the water-insoluble TEMPO-oxidized products. Although the dispersion for the TEMPO-oxidized tubeworm  $\beta$ -chitin prepared with 20 mmol NaClO per gram of chitin was highly transparent, the yield of the water-insoluble fraction was only about 16% in this case (Fig. 1). Thus, the TEMPO-oxidized tubeworm  $\beta$ -chitins prepared with either 5.0 or 10 mmol NaClO per gram of chitin

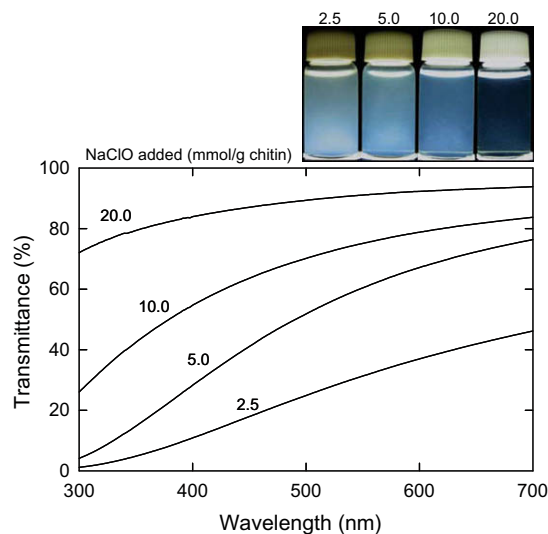


**Fig. 7.** UV-visible light-transmittance spectra for the 0.1% aqueous dispersions of TEMPO-oxidized tubeworm  $\beta$ -chitins prepared with different NaClO addition levels and photographs of the corresponding dispersions.

are suitable for preparation of homogeneously dispersed and translucent (not transparent) gels from the water-insoluble fractions by disintegration in water.

### 3.5. TEM observation of TEMPO-oxidized tubeworm $\beta$ -chitin nanofibrils

Transmission electron microphotographs (TEM) of the dispersion of the water-insoluble fraction of TEMPO-oxidized tubeworm  $\beta$ -chitin prepared with 10 mmol NaClO per gram of chitin are observed after drying (Fig. 8). Long TEMPO-oxidized tubeworm  $\beta$ -chitin nanofibrils were clearly observed, and had widths ranging 20–50 nm and lengths of more than several microns. Thus, although the dispersions were not completely transparent but only translucent, the tubeworm  $\beta$ -chitin fibrils were mostly converted to highly crystalline and individual nanofibrils dispersed in water by the TEMPO-mediated oxidation and the following mechanical disintegration.

As shown by one of the white arrows in the upper TEM image of Fig. 8, the fibril had a twisted part, indicating that each fibril has a flat and ribbon-like morphology 20–50 nm in width and ca. 15 nm in thickness. Another white arrow in Fig. 8 shows an edge of the nanofibrils probably formed by scission during disintegration in water. Because each individual nanofibril in Fig. 8 had a clear electron diffraction spots at any locations, one TEMPO-oxidized tubeworm  $\beta$ -chitin nanofibril does not consist of multiple elementary fibrils but forms a perfect crystallite.

Fig. 9 shows changes in the weight ratio of the water-insoluble fraction from Fig. 1, the fibril width determined from TEM images and the crystal sizes to the (110) and (100) directions determined from X-ray diffraction patterns in Fig. 2 for the TEMPO-oxidized tubeworm  $\beta$ -chitins prepared with different NaClO addition levels. Even though the fibril widths determined from TEM images had large deviations, the decreasing pattern of the fibril width with increasing the NaClO addition level is correlated well to that of the weight ratio of the water-insoluble fraction in the range of 2.5–10 mmol NaClO per gram of the tubeworm  $\beta$ -chitin. The average widths were 39.6 nm, 30.0 nm and 26.4 nm, when the TEMPO-oxidized  $\beta$ -chitins were prepared with NaClO of 2.5 mmol, 5.0 mmol and 10 mmol per gram of chitin, respectively. At least in the NaClO addition range of 2.5–10 mmol/g, the oxida-

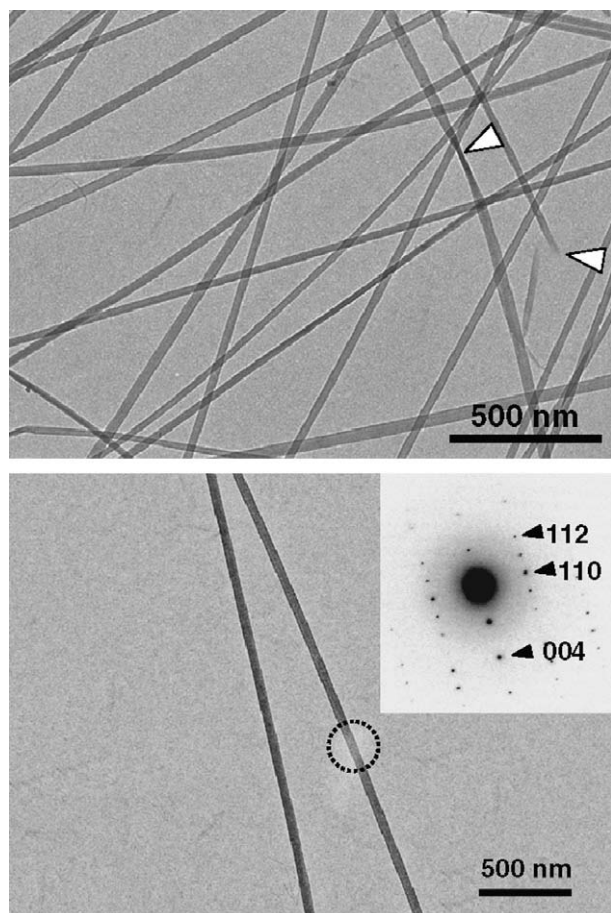


**Fig. 8.** Transmission electron microphotographs and electron diffraction diagram of nanofibrils of TEMPO-oxidized tubeworm  $\beta$ -chitin prepared with 10 mmol NaClO per gram of chitin. White arrows show twisted and cut parts of the fibrils.

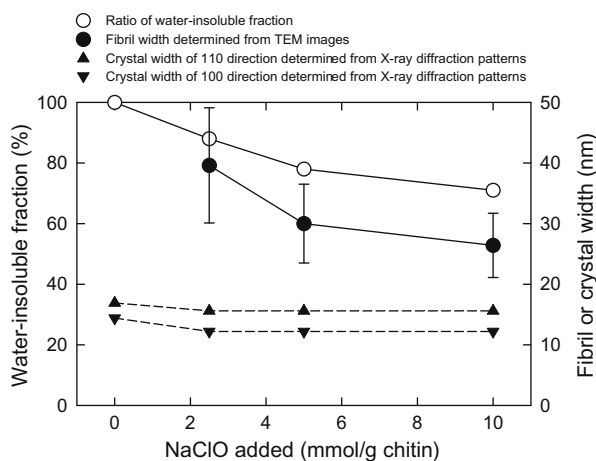


**Fig. 9.** Changes in the weight ratio of water-insoluble fraction, fibril width determined by TEM images and crystal sizes determined by X-ray diffraction patterns for the TEMPO-oxidized tubeworm  $\beta$ -chitin by the NaClO addition level.

tion of chitin molecules to water-soluble chitouronic acids takes place from each edge of the fibril width to inside crystallites. These chitouronic acid molecules formed are dissolved in the aqueous oxidation media, and removed from the fibril surfaces like peeling-off behavior during the TEMPO-mediated oxidation,

resulting in the decrease in the fibril width with increasing the NaClO addition.

However, the fibril widths of the TEMPO-oxidized tubeworm  $\beta$ -chitin nanofibrils observed by TEM in Fig. 8 were always larger than the (110) and (100) crystal sizes determined from X-ray diffraction patterns of the water-insoluble TEMPO-oxidized tubeworm  $\beta$ -chitins. Moreover, the crystal sizes were nearly unchanged to the NaClO addition level in the range of 2.5–10 mmol/g; the decreasing pattern of fibril width determined from TEM images did not correlated to the patterns of crystal sizes. As described previously, the TEMPO-oxidized tubeworm  $\beta$ -chitin nanofibrils have flat and ribbon-like morphologies. Probably, only the diffraction planes parallel to the surfaces of the ribbon-like TEMPO-oxidized tubeworm nanofibrils observed in Fig. 8 are detectable as X-ray diffraction peaks. This is because the flat and ribbon-like nanofibrils are packed in parallel manner to the surface of the sample pellets prepared by pressing and subjected to the reflection-type X-ray diffraction analysis. X-ray diffraction can provide only information to the thickness direction of the flat and ribbon-like nanofibrils, while TEM images provide the width information of the nanofibrils. Thus, the discrepancy between the fibril widths determined from TEM images and the crystal sizes determined by X-ray diffraction patterns in Fig. 9 is likely to be caused by the flat and ribbon-like morphology of tubeworm  $\beta$ -chitin fibrils.

Based on the above results, chitin molecules in the flat and ribbon-like fibrils are oxidized from each edge of the fibril width in Fig. 8 to inside crystallites, forming water-soluble chitouronic acid molecules, as the NaClO addition level increases in the TEMPO-mediated oxidation. Consequently, the width of the fibrils decreases with the NaClO addition. On the other hand, the thickness of the fibrils is maintained during the oxidation; chitin molecules are not removed as chitouronic acids from the upper or lower sides of the flat and ribbon-like fibrils in Fig. 8.

#### 4. Conclusions

In the case of squid pen  $\beta$ -chitin, although the water-insoluble fractions were obtained from the TEMPO-oxidized products by controlling the NaClO addition level, the oxidized products could not be converted to individual nanofibrils under any conditions examined so far by disintegration in water. On the other hand, when tubeworm  $\beta$ -chitin was oxidized by the TEMPO-mediated system with 2.5–10 mmol NaClO per gram of chitin, the water-insoluble fractions with carboxylate contents of 0.18–0.25 mmol/g were obtained in the yields of more than 70%. X-ray diffraction, solid-state  $^{13}\text{C}$ -NMR and FT-IR analyses revealed that the water-insoluble TEMPO-oxidized tubeworm  $\beta$ -chitins had crystallinity indices, crystal sizes and degrees of N-acetylation quite similar to those of the original  $\beta$ -chitin. Nearly no aldehyde groups were present in the water-insoluble fractions. Homogeneous, highly viscous and translucent (not transparent) gels can be obtained by disintegration of the above water-insoluble TEMPO-oxidized tubeworm  $\beta$ -chitins in water. The gels consist of nanofibrils 20–50 nm in width and at least several microns in length. Thus, the carboxylate groups formed by the TEMPO-mediated oxidation are likely to be present selectively on the tubeworm  $\beta$ -chitin fibril surfaces. TEM images of the TEMPO-oxidized tubeworm showed that each fibril had the flat and ribbon-like morphology. As the NaClO addition level increased, the widths of nanofibrils were decreased by peeling-off of chitin molecules as water-soluble chitouronic acid molecules in the aqueous oxidation media. When sufficient amounts of NaClO were used, both tubeworm and squid pen  $\beta$ -chitins are mostly converted to water-soluble chitouronic acid Na salts by complete oxidation of the C6 primary hydroxyls to carboxyl groups.

## Acknowledgements

This research was supported by Grant-in-Aids for Scientific Research (Grant Nos. 18380102 and 18-10902) from the Japan Society for the Promotion of Science (JSPS). Y.M.F. is a recipient of the Monbu-Kagakusho Fellowship for foreign students. Dr. Masahisa Wada and Dr. Yutaka Yoshida of University of Tokyo kindly provided tubeworm samples and measured the solid-state  $^{13}\text{C}$ -NMR spectra. Mr. Zhiguo Wang of University of Tokyo helped us to take the photographs of dispersion and suspension samples.

## References

- Alexander, L. E. (1979). *X-ray diffraction methods in polymer science*. New York: Krieger.
- Blackwell, J. (1988). Physical methods for the determination of chitin structure and conformation. *Methods in Enzymology*, 161, 435–442.
- Fan, Y. M., Saito, T., & Isogai, A. (2008a). Chitin nanocrystals prepared by TEMPO-mediated oxidation of  $\alpha$ -chitin. *Biomacromolecules*, 9, 192–198.
- Fan, Y. M., Saito, T., & Isogai, A. (2008b). Preparation of chitin nanofibers from squid pen  $\beta$ -chitin by simple mechanical treatment under acid conditions. *Biomacromolecules*, 9, 1919–1923.
- Goodrich, J. D., & Winter, W. T. (2007).  $\alpha$ -Chitin nanocrystals prepared from shrimp shells and their specific surface area measurement. *Biomacromolecules*, 8, 252–257.
- Imai, T., Watanabe, T., Yui, T., & Sugiyama, J. (2003). The directionality of chitin biosynthesis: a revisit. *The Biochemical Journal*, 374, 755–760.
- Kato, Y., Kaminaga, J., Matsuo, R., & Isogai, A. (2004). TEMPO-mediated oxidation of chitin, regenerated chitin and N-acetylated chitosan. *Carbohydrate Polymers*, 58, 421–426.
- Kurita, K. (2001). Controlled functionalization of the polysaccharide chitin. *Progress in Polymer Science*, 26, 1921–1971.
- Li, J., Revol, J.-F., & Marchessault, R. H. (1997). Effect of degree of deacetylation of chitin on the properties of chitin crystallites. *Journal of Applied Polymer Science*, 65, 373–380.
- Lu, Y., Weng, L., & Zhang, L. (2004). Morphology and properties of soy protein isolate thermoplastics reinforced with chitin whiskers. *Biomacromolecules*, 5, 1046–1051.
- Mazeau, K., Winter, W. T., & Chanzy, H. (1994). Molecular and crystal structure of a high-temperature polymorph of chitosan from electron diffraction data. *Macromolecules*, 27, 7606–7612.
- Morin, A., & Dufresne, A. (2002). Nanocomposites of chitin whiskers from Riftia tubes and poly(caprolactone). *Macromolecules*, 35, 2190–2199.
- Muzzarelli, R. A. A. (1977). *Chitin*. Oxford: Pergamon.
- Muzzarelli, R. A. A., Muzzarelli, C., Cosani, A., & Terbojevich, M. (1999). 6-Oxichitons, novel hyaluronan-like regiospecifically carboxylated chitins. *Carbohydrate Polymers*, 39, 361–367.
- Muzzarelli, R. A. A., Morganti, P., Morganti, G., Palombo, P., Palombo, M., Biagini, G., et al. (2007). Chitin nanofibrils/chitosan glycolate composites as wound medicaments. *Carbohydrate polymer*, 70, 274–284.
- Paillet, M., & Dufresne, A. (2001). Chitin whisker reinforced thermoplastic nanocomposites. *Macromolecules*, 34, 6527–6530.
- Peersen, O. B., Wu, X., Kustanovich, I., & Smith, S. O. (1993). Variable-amplitude cross-polarization MAS NMR. *Journal of Magnetic Resonance Series A*, 104, 334–339.
- Revol, J.-F., & Marchessault, R. H. (1993). In-vitro chiral nematic ordering of chitin crystallites. *International Journal of Biological Macromolecules*, 15, 329–335.
- Saito, T., & Isogai, A. (2004). TEMPO-mediated oxidation of native cellulose. The effect of oxidation conditions on chemical and crystal structures of the water-insoluble fractions. *Biomacromolecules*, 5, 1983–1989.
- Saito, T., Kimura, S., Nishiyama, Y., & Isogai, A. (2007). Cellulose nanofibers prepared by TEMPO-mediated oxidation of native cellulose. *Biomacromolecules*, 8, 2485–2491.
- Saito, Y., Kumagai, H., Wada, M., & Kuga, S. (2002). Thermally reversible hydration of  $\beta$ -chitin. *Biomacromolecules*, 3, 407–410.
- Saito, T., Nishiyama, Y., Putaux, J. L., Vignon, M., & Isogai, A. (2006). Homogeneous suspensions of individualized microfibrils from TEMPO-catalyzed oxidation of native cellulose. *Biomacromolecules*, 7, 1687–1691.
- Shigemasa, Y., Matsuura, H., Sashiwa, H., & Saimoto, H. (1996). Evaluation of different absorbance ratios from infrared spectroscopy for analyzing the degree of deacetylation in chitin. *International Journal of Biological Macromolecules*, 18, 237–242.